Available online at www.sciencedirect.com
SCIENCE DIRECT®
Antiviral Research 63 (2004) 107–113
Antiviral Research
www.elsevier.com/locate/antiviral

Intracellular metabolism and pharmacokinetics of 5′-hydrogenphosphonate of 3′-azido-2′,3′-dideoxythymidine, a prodrug of 3′-azido-2′,3′-dideoxythymidine

Yurii Skoblov [a], Inna Karpenko [a], Elena Shirokova [a], Konstantin Popov [a], Valerya Andronova [b], Georgii Galegov [b], Marina Kukhanova [a,*]

[a] *Engelhardt Institute of Molecular Biology, RAS, 32 Vavilov St., 119991 Moscow, Russian Federation, Russia*
[b] *Ivanovsky Institute of Virology, RAMS, 16 Gamalei St., 123098 Moscow, Russian Federation, Russia*

Received 20 October 2003; accepted 25 March 2004

Abstract

5′-Hydrogenphosphonate of 3′-azido-2′,3′-dideoxythymidine (HpAZT), a novel anti-HIV drug approved for the treatment of HIV-infected patients in Russia, displays some clinical advantages over azidothymidine (AZT). Metabolism in the HL-60 cell culture and pharmacokinetics in mice of [6-^{3}H]-HpAZT (in comparison with [6-^{3}H]-AZT) were studied to elucidate the metabolic basis of its lower clinical toxicity. Accumulation of [6-^{3}H]-HpAZT-derived products in cells with time, distribution of its radioactive metabolites among blood and different mouse organs and dependence of drug accumulation on the route of administration were investigated. The rate of accumulation of [^{3}H]-HpAZT metabolites in cells was slower than the rate of accumulation of [^{3}H]-AZT metabolites. [^{3}H]-AZTMP was the dominating metabolite at all time points, achieving the level of 15 ± 3 pmol/10^6 cells after 25 h incubation. After oral or intravenous administrations of [^{3}H]-HpAZT, the (radioactive) metabolites were rapidly distributed among blood, stomach, intestine and liver and were not found in brain, muscles and spleen. [^{3}H]-HpAZT underwent rapid and extensive metabolism, [^{3}H]-AZT being the dominating product at all time points. Administration of 180 nmol of [^{3}H]-HpAZT resulted in an AZT concentration in blood of 1–3 μM after 5 min, which remained practically constant during the next 25 min and did not depend on the route of administration.

Keywords: Metabolism; Pharmacokinetics; HIV inhibitors; 5′-Hydrogenphosphonate of azidothymidine

1. Introduction

Azidothymidine (AZT) is a potent inhibitor of HIV replication and the first clinically approved drug for AIDS (Yarchoan et al., 1986). The major limitations of AZT chemotherapy are clinical toxicity that includes dose-related bone marrow suppression manifested as severe anaemia and leucopenia (Richman et al., 1987), hepatic abnormalities, myopathy (Chariot et al., 1999), limited brain uptake (Grootuis and Levy, 1997), a short half-life in plasma (Girard et al., 2000) and the rapid development of virus–drug resistance (Kellam et al., 1992; Ren et al., 1998). Pharmacokinetic studies in humans have shown that the AZT plasma half-life is approximately 1 h (Klecker et al., 1987). This necessitates administration of higher doses for maintaining therapeutic drug levels in plasma, thus leading to bone marrow toxicity. Therefore, it was reasoned that AZT in prodrug forms may significantly overcome the drawbacks of AZT, improve its efficacy and decrease its adverse effects. Successful prodrugs are expected to possess good stability in plasma, and yet generate therapeutically effective levels of AZT in the target organs.

Several research groups have reported synthesis of various types of conjugates of AZT with amino acids, retinoic acid, lipids and others (Aggarwal et al., 1990; McGuigan et al., 1990; Piantadosi et al., 1991). These prodrugs have been designed to improve the AZT pharmacokinetic profile or to directly deliver AZTMP, and thus to overcome the problem of poor monophosphorylation. In comparison to AZT, some of the prodrugs showed similar anti-HIV activity with considerably improved pharmacokinetic properties and decreased toxicity. Among AZT prodrugs, 5′-hydrogenphosphonate of AZT (HpAZT) was reported to exhibit a potent anti-HIV activity with the selectivity index similar to or better than

* Corresponding author. Tel.: +7-95-135-2255; fax: +7-95-135-1405.
E-mail address: kukhan86@hotmail.com (M. Kukhanova).

0166-3542/$ – see front matter © 2004 Elsevier B.V. All rights reserved.
doi:10.1016/j.antiviral.2004.03.001

that of the parent AZT (Khorlin et al., 1992; Wainberg et al., 1992; Gosselin et al., 1993; Machado et al., 1999).

HpAZT (Nicavir®) was approved by the Russian Ministry of Health for the treatment of HIV-infected patients in 1999. The main advantages of HpAZT over AZT include its lower toxicity, a longer half-life in organism, and much slower selection for virus-drug resistance (Wainberg et al., 1998). HpAZT can be used for the treatment of HIV-infected patients with the history of AZT intolerance (Yurin et al., 2001). Recently, the combined therapy including HpAZT, Videx and nevirapin was shown to be effective and safe and was recommended for the treatment of HIV-infected persons in Russia (Kravchenko et al., 2001).

Here, the [6-^{3}H]-HpAZT metabolism and the rate of accumulation of its metabolites in the HL-60 cell line relative to that of [6-^{3}H]-AZT are reported. Also, the data on pharmacokinetics in mice after oral or intravenous (i.v.) administration of [6-^{3}H]-HpAZT and the distribution of its radiolabelled metabolites among different mouse organs and blood are presented in comparison to those of [6-^{3}H]-AZT.

2. Material and methods

2.1. Materials

Non-labelled AZT was a kind gift from "AZT Association" (Moscow, Russia). [6-^{3}H]-AZT (19 Ci/mmol) was synthesised according to a published procedure (Sidorov et al., 2003). [6-^{3}H]-HpAZT was synthesised similar to the method described for the non-labelled HpAZT (Khorlin et al., 1992). A promyelocyte cell line HL-60 (ATCC CCL-240) was cultured in RPMI 1640 medium (Sigma, St. Louis, MO) supplemented with 10% fetal calf serum (FCS) (Seromed, Germany). HPLC analysis of cellular metabolites was performed using a Gilson HPLC system 311 (France) supplemented with Model 303 solvent pumps and a UV-detector.

2.2. Analysis of [^{3}H]-HpAZT and [^{3}H]-AZT metabolites in cell culture

Metabolism of [^{3}H]-HpAZT in the HL-60 cell culture was studied according to a previously established procedure (Balzarini et al., 1991). Briefly, 4 ml of the HL-60 cell suspensions at (0.6–0.8) $\times$ 10^6 cells/ml in the RPMI 1640 culture medium supplemented with 10% FCS were incubated with 25 μM (10 μCi) [^{3}H]-HpAZT or [^{3}H]-AZT in 4 cm dishes. At certain time intervals (0, 1, 3, 7, 25 h), the cells were collected by centrifugation at 800 $\times$ *g* for 5 min. The supernatant was analysed by reversed-phase HPLC to reveal degradation of the compounds in the cell medium. The cell pellets were washed four times with a cold phosphate saline buffer (PBS, pH 7.4) and the products were extracted by 60% ice-cold methanol. After 30 min at −20 °C, the suspension was centrifuged for 30 min at 15,000 $\times$ *g*, and the aliquots of the supernatant were assayed for the amount of radioactivity in a liquid scintillation counter. The remaining supernatant was dried in a Speed-Vac centrifuge, the pellets were reconstituted in 100 μl of deionized water and stored at −20 °C. After thawing, 15 μl aliquots were subjected to HPLC analysis.

2.3. HPLC analysis of [^{3}H]-HpAZT and [^{3}H]-AZT metabolites

Intracellular metabolites of [^{3}H]-HpAZT or [^{3}H]-AZT were analysed by reversed-phase HPLC using a Lichrosorb C18 (7 μm, 4 mm $\times$ 150 mm) column preceded by a guard C2 column (45 μm, 4 mm $\times$ 20 mm). The mobile phase consisted of two buffers: A (50 mM triethylammonium bicarbonate, pH = 7.5), and B (70% ethanol). Elution was performed at a constant flow rate of 0.5 ml/min using a multistage gradient beginning with 0% buffer B that was maintained for 5 min and was subsequently increased to 10% during 10 min, to 25% during 25 min, to 30% during 37 min, and reached 100% at 40 min. The radiolabelled products were identified by the comparison of their retention times with those of unlabelled authentic thymidine, AZT, AZTMP and HpAZT (7.5, 28, 17.5 and 24 min, respectively). Additionally, to these derivatives, unidentified metabolites, designated as M1, were eluted at 1–3 min. Phosphorylated products were analysed using a Partisil SAX anion exchanged column (Whatman). A linear gradient of phosphate buffer (0–1.0 M, pH 7.0) was used as a mobile phase.

2.4. Animal study

Albino laboratory mice weighing 15–20 g were used for oral or i.v. administration of [^{3}H]-HpAZT or [^{3}H]-AZT. Three mice in each group were taken for these experiments. The mice received 300 μCi orally or 20 μCi intravenously of the drugs ([^{3}H]-HpAZT or [^{3}H]-AZT), the total amount of the administered compounds being 180 nmol. At certain time intervals postadministration (2, 6, 12, 20 min), mice were sacrificed by CO_2 asphyxiation. The blood samples were collected by heart puncture. Several organs including liver, kidneys, spleen, muscles, stomach, small and large intestines were collected and weighed. The organs were homogenised in PBS, the suspensions were centrifuged at 5000 $\times$ *g* for 10 min, and aliquots of the supernatants were assayed in a liquid scintillation counter. Identification of the radioactive metabolites and their relative amounts were carried out by reversed-phase HPLC as described above.

2.5. Hydrolysis of [^{3}H]-HpAZT in mouse liver homogenates

Mouse liver was homogenised in four volumes of PBS and centrifuged at 3000 $\times$ *g* for 10 min. The supernatant fraction was used for the experiments. Incubation mixture contained in a total volume of 100 μl: 2 μCi (12 μM) [^{3}H]-HpAZT, 2 mM $MgCI_2$, 1.7 mg/ml liver supernatant fraction, and PBS.

Samples of 15 μl were taken at different time intervals, and three volumes of methanol were added. After 20 min at −20 °C, the pellets were precipitated by centrifugation at 15,000 × *g* for 5 min and aliquots of the supernatant were analysed by HPLC.

2.6. Hydrolysis of [^{3}H]-HpAZT in cellular extracts

HL-60 cells (2×10^7) were washed twice with PBS and disintegrated by cryolysis. The suspension was centrifuged at 3000 × *g* for 10 min, and the supernatant was used for the experiments. Reaction mixtures contained the same components as described in Section 2.5.

3. Results

3.1. Metabolism of [^{3}H]-HpAZT in the HL-60 cell culture

HL-60 cells (3×10^6) were exposed to 25 μM (10 μCi) [^{3}H]-HpAZT or [^{3}H]-AZT for 0, 1, 3, 7 and 25 h. Fig. 1A shows the time-dependent accumulation of the radioactive products in cells after their incubation with either [^{3}H]-HpAZT (1) or [^{3}H]-AZT (2). The amount of radioactive intracellular HpAZT metabolites was 20–30% when compared with that for [^{3}H]-AZT for the first 5 h. Then, the amount of intracellular [^{3}H]-HpAZT- derived products gradually increased and attained 50–60% of that of AZT after a 25 h incubation. Intracellular metabolites after incubation with either [^{3}H]-HpAZT or [^{3}H]-AZT were analysed by reversed-phase HPLC as described in Section 2. Identification of the radiolabelled compounds was based on their co-elution with non-radioactive authentic thymidine, AZT, AZTMP and HpAZT. HPLC analysis of intracellular radioactive products showed (Fig. 1B) that after one hour of the exposure of cell culture to HpAZT, the HpAZT amount constituted only several percents of the total amount of intracellular radiolabelled metabolites and remained practically constant for the remaining time of the experiment (4). This implies that HpAZT was rapidly metabolised inside the cells. The amount of the dominating metabolite, AZTMP, achieved 20 ± 5 pmol/10^{6}cells (80 ± 15% of the total radioactivity) after a 25 h incubation with HpAZT (2), that was almost three times lower in comparison with the experiments where AZT was used (1). Surprisingly, only a small amount of AZT (3) was found among the cellular metabolites after the cell incubation with HpAZT. As was revealed by anion exchange chromatography, AZTDP or AZTTTP amounted to as little as 0.1–0.2% of the total intracellular radioactivity (data not shown). Neither [^{3}H]-thymine nor [^{3}H]-thymidine were found among the cellular metabolites. These results imply that [^{3}H]-HpAZT was either hydrolysed to AZT followed by its phosphorylation to AZTMP, or was directly oxidised to give [^{3}H]-AZTMP, or both. Less than 0.1% of radioactivity was also found in the methanol-insoluble fraction.

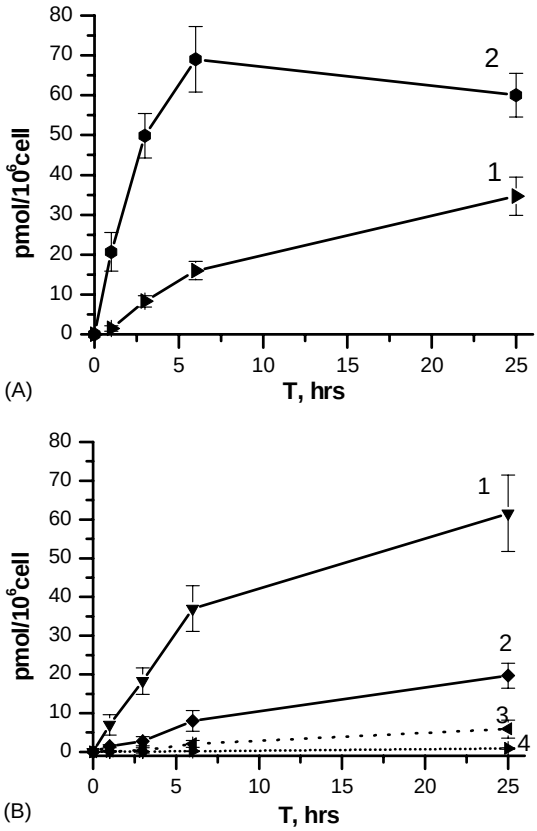

Fig. 1. (A) Time-dependent intracellular accumulation of radioactive metabolites in HL-60 cells during incubation of 3×10^6 cells with 25 μM (10 μCi) of (1) [^{3}H]-HpAZT or (2) [^{3}H]-AZT. The 15 μl aliquots of methanol-soluble cellular extracts were counted in a liquid scintillation counter. (B) Intracellular radioactive metabolites generated in HL-60 cells exposed to [^{3}H]-AZT or [^{3}H]-HpAZT (see A). Identification of metabolites in the methanol-soluble extracts was carried out by reversed-phase HPLC, as described in Section 2. Metabolites: [^{3}H]-AZTMP after incubation with (1) [^{3}H]-AZT or (2) [^{3}H]-HpAZT, respectively; [^{3}H]-AZT after incubation with (3) [^{3}H]-HpAZT; the amount of (4) [^{3}H]-HpAZT. Each value is the mean ± S.D. from three determinations.

3.2. Hydrolysis of [^{3}H]-HpAZT in cell media, total cellular extracts and liver homogenates

Decomposition pathways of HpAZT in a total cellular extract and crude mouse liver homogenate were studied. Additionally, HpAZT hydrolysis was investigated in the RPMI 1640 medium containing 10% FCS in order to differentiate chemical and enzymatic hydrolysis. After incubation of the reaction mixtures at 37 °C for certain time intervals, the aliquots were analysed by HPLC. Fig. 2 demonstrates [^{3}H]-HpAZT hydrolysis upon its incubation in HL-60 cellular extracts (1). [^{3}H]-HpAZT was hydrolysed by 40% after the 1.5 h incubation to give two products [^{3}H]-AZT (2) and [^{3}H]-AZTMP (3) in a ratio of 3.5:1. It should be noted that HpAZT was stable in the RPMI medium supplemented with 10% FCS during the experimental time (4). Only 10–15% of HpAZT were converted to AZT after the 25 h incubation at 37 °C (data not shown). Fig. 3 presents the results of

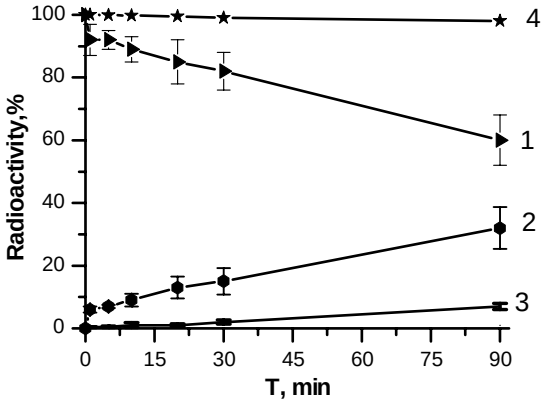

Fig. 2. Time-dependent (1) hydrolysis of [^{3}H]-HpAZT in HL-60 cellular extract, (2) accumulation of [^{3}H]-AZT and (3) [^{3}H]- AZTMP. (4) Stability of HpAZT in RPMI 1640 medium supplemented by 10% FCS. A total amount of radioactivity in the sample was taken as 100%. Conditions of the experiments are described in Section 2. Each value is the mean ± S.D. from three determinations.

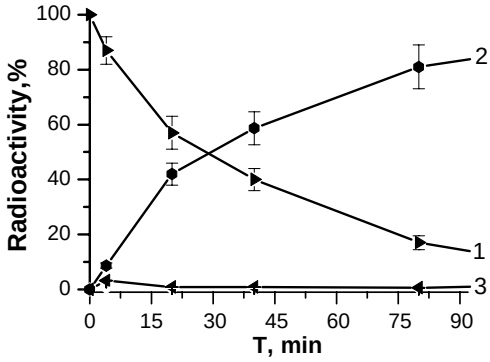

Fig. 3. Time-dependent (1) hydrolysis of [^{3}H]-HpAZT, (2) accumulation of [^{3}H]-AZT and (3) [^{3}H]- AZTMP in crude mouse liver homogenate. A total amount of radioactivity in the sample was taken as 100%. Each value is the mean ± S.D. from three determinations. Conditions of the experiments are described in Section 2.

[^{3}H]-HpAZT hydrolysis in mouse liver homogenate. The half-life of [^{3}H]-HpAZT (1) was about 30 min. It means that the activity of hydrolysing enzymes in the liver homogenate was higher than that in cellular extracts. Hydrolysis of [^{3}H]-HpAZT gave rise to [^{3}H]-AZT (2), which is a prevailing product; only a little amount of another radioactive metabolite was found that was identified as [^{3}H]-AZTMP (3). The differences in the efficacy of HpAZT conversion into AZTMP in cells (Fig. 1B) and the data shown in Figs. 2 and 3 could be explained by the higher activity of nucleoside kinases in cells relative to cellular or liver extracts.

3.3. The distribution of [^{3}H]-HpAZT metabolites among mouse organs and blood after oral administration

Fig. 4 shows the distribution of [^{3}H]-HpAZT-derived metabolites among mouse blood and organs just after oral administration (panel A) and 20 min later (panel B) in comparison with that of [^{3}H]-AZT (panels C and D, respectively). Two minutes post administration of [^{3}H]-HpAZT,

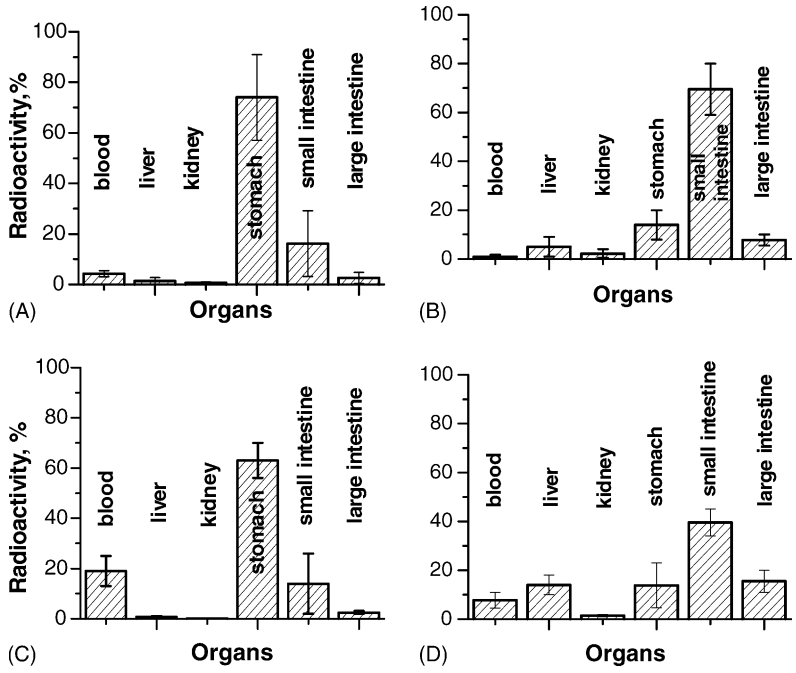

Fig. 4. The distribution of radiolabelled metabolites among mouse organs and blood (A, C) 2 min and (B, D) 20 min later after oral administration of 180 nmol (300 μCi) of (A, B) [^{3}H]-HpAZT or (C, D) [^{3}H]-AZT. A total amount of radioactivity in the organ or blood was taken as 100%. Each value is the mean ± S.D. from two independent determinations. Conditions of the experiments are described in Section 2.

80–90% of total radioactive metabolites were found in stomach and about 5% in blood. The amount of radioactivity in blood corresponded to a 8–10 μM concentration of the drug and/or its metabolites. After 20 min (Fig. 4B), the amount of radioactive products in blood was decreased by 5 times, achieving a 1–2 μM concentration. The remaining radioactive HpAZT-derived products were distributed among stomach (15–20%), small intestine (60%), liver, kidneys and large intestine (about 5–8% in each organ). No radioactivity was found in brain, muscles and spleen during the experimental time. HPLC analysis of radioactive products in mouse blood and organs showed that the major part of radioactivity after the HpAZT administration was accounted as [^{3}H]-AZT in all time points of the experiment. Small amounts of [^{3}H]-HpAZT and [^{3}H]-AZTMP were detected in stomach (data not shown). Fig. 4C and D demonstrate the results for similar experiments with [^{3}H]-AZT. Distribution of radioactive metabolites among mouse organs did not differ much from that of [^{3}H]-HpAZT. However, 2 min post administration of [^{3}H]-AZT (Fig. 4C), the concentration of radioactive products in blood was two to four-fold higher if compared with that of [^{3}H]-HpAZT (Fig. 4A). After 20 min, the concentration of [^{3}H]-AZT-derived products was decreased twice (Fig. 4D), but still remained higher than in the case of [^{3}H]-HpAZT (Fig. 4B). Non-identified metabolic products (M1), whose retention times were 1–3 min, were mainly found in liver. Fig. 5 presents the accumulation of radioactive M1 products in mouse liver after [^{3}H]-HpAZT administration. After 5 min, they constituted 80 ± 10% of the total amount of radioactive products in liver. Small

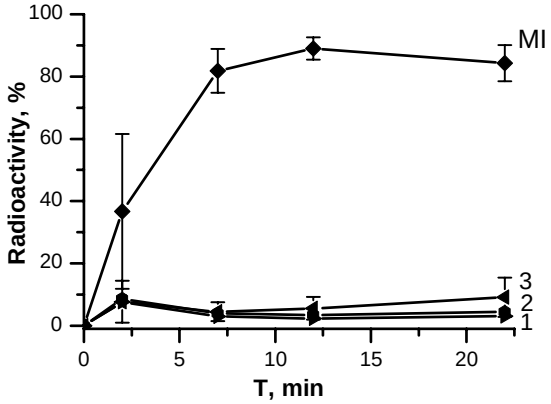

Fig. 5. Time-dependent accumulation of [^{3}H]-HpAZT-derived metabolites in mouse liver after oral drug administration. Mouse liver was homogenised and after centrifugation the methanol-soluble fraction of the supernatant was subjected to reversed-phase HPLC, as described in Section 2. Non-identified metabolites (M1), (1) HpAZT, (2) AZTMP and (3) AZT. Each value is the mean ± S.D. from three determinations.

amounts of HpAZT (1), AZTMP (2) and AZT (3) were also detected among the radioactive products.

3.4. Distribution of [^{3}H]-HpAZT metabolites among mouse organs and blood after i.v. administration

Fig. 6 shows the distribution of [^{3}H]-HpAZT-derived metabolites (A, B) among mouse blood and organs after i.v. administration in comparison with that of [^{3}H]-AZT (C, D). One can see that 2 min after the drug application,

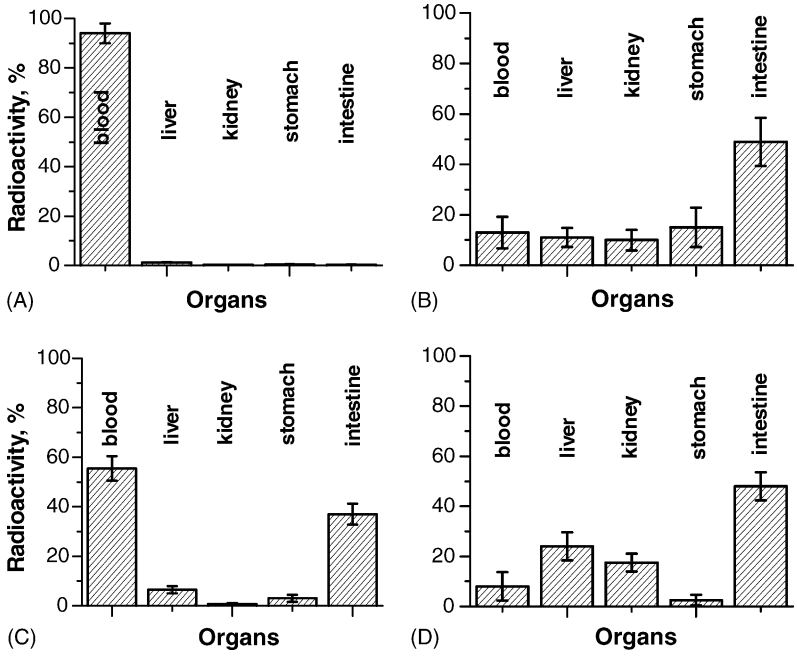

Fig. 6. The distribution of radiolabelled metabolites among mouse organs and blood (A, C) 2 min and (B, D) 20 min later after i.v. administration of 180 nmol (20 μCi) of (A, B) [^{3}H]-HpAZT or (C, D) [^{3}H]-AZT. A total amount of radioactivity in the organ or blood was taken as 100%. Conditions of the experiments are described in Section 2. Each value is the mean ± S.D. from two independent determinations.

98% of [^{3}H]-HpAZT metabolites were found in blood (A) whereas 10 min later the amount of radioactivity in blood dropped almost 10 times (B). The residual radioactivity was distributed among intestine (40–50%), liver, kidneys and stomach (about 10–15% in each organ). The HPLC analysis of radioactive products showed that the radioactive material(s) after HpAZT administration were accounted for by [^{3}H]-AZT in any time point of the experiment. When [^{3}H]-AZT was used as a drug, the distribution of AZT metabolites (D) was similar to that of HpAZT (B) 10 min post administration. Some differences between the distribution of AZT and HpAZT among mouse organs were noted 2 min later after the drug administration. The amount of radioactive metabolites in blood was lower and in stomach much higher (C) after AZT application if compared with that when [^{3}H]-HpAZT (A) was used. An elevated concentration of radioactivity was found in liver and kidneys (D). This indicates that AZT metabolism in mouse is more extensive than that of HpAZT.

4. Discussion

A variety of AZT prodrugs have been investigated to circumvent some of the limitations associated with AZT therapy such as dose-dependent bone marrow toxicity, short half-life in organism, inability to penetrate into brain, and dependence on cellular phosphorylating enzymes (Aggarwal et al., 1990; Vlieghe et al., 2001; Bonina et al., 2002; Perigaud et al., 1997; McGuigan et al., 1996; Zemlicka, 2002; Wagner et al., 2000). Phosphorus-containing groups of nucleotide analogues are the basis for the design of new repertoire of nucleoside-based antiviral drugs. It was reported that HpAZT might be an attractive anti-HIV drug (Khorlin et al., 1992; Wainberg et al., 1998; Machado et al., 1999). HpAZT has structural similarities to AZTMP but, unlike AZTMP, might be resistant to extra and/or intracellular dephosphorylation and could penetrate through cellular membranes due to its less polar nature. It might function as an AZT prodrug or be directly oxidised to AZTMP. HpAZT has been approved (in Russia) for the treatment of HIV-infected patients. According to the clinical data, the advantages of HpAZT over AZT are lower toxicity and longer half-life in organism. The study of accumulation of HpAZT-derived metabolites in dog blood showed that HpAZT was rapidly converted into AZT after oral administration. The comparative dynamics of AZT accumulation in dog blood after oral HpAZT and AZT administration revealed the following. First, the highest concentrations of AZT in dog blood were achieved at 6 and 3 h after HpAZT or AZT administration, respectively. Second, the highest AZT concentration reached after HpAZT administration was more than three times lower than that after AZT administration (Kononov A.V., personal information).

Here, we studied metabolism in cell culture and pharmacokinetics in mice of radiolabelled [6-H^3]-HpAZT relatively to [6-^{3}H]-AZT. We showed that the accumulation rate of radioactive products in cells after their exposure to [H^3]-HpAZT was lower than that of [^{3}H]-AZT. HPLC analysis of intracellular radioactive products showed that AZTMP was a predominant product at all experimental time points. Only a few percents of AZT and HpAZT were detected inside the cells. These results correlated with the previously published data (Boal et al., 1993), where it was suggested that HpAZT was converted into AZTMP by oxidation. However, incubation of [H^3]-HpAZT with crude HL-60 cellular extracts or mouse liver homogenate demonstrated that AZT was a major metabolic product. AZTMP was also found, but only in lower amounts are compared with the amount of AZTMP found in cells exposed to AZT. Most probably, HpAZT was hydrolysed during its penetration through cellular membranes by membrane-associated exonucleases or by 5′-nucleotidases just after its penetration into cells followed by phosphorylation to AZTMP (Fig. 1B). However, we cannot exclude the possibility of direct oxidation of HpAZT to AZTMP in some cell cultures. The reduced accumulation of AZTMP after incubation of cells with HpAZT (Fig. 1B) could explain lower cellular toxicity of HpAZT compared with that when AZT was used as a drug. It was shown (Tornevik et al., 1995) that the cellular toxicity was associated with a high concentration of AZTMP, which inhibited thymidine/thymidylate kinases and caused nucleoside imbalance in cells. The animal study demonstrated that HpAZT was rapidly converted into AZT in vivo after oral or i.v. administration into mice, thus being an AZT prodrug. The amount of [^{3}H]-HpAZT-derived metabolites in mouse blood did not depend on the type of administration except for the first minutes after i.v. administration when all radioactivity was found in blood. The concentration of AZT in blood after administration of 180 nmol of [^{3}H]-HpAZT was 1–2 μM. The distribution of [H^3]-HpAZT-derived metabolites among mouse blood, liver, kidneys, large and small intestine did not differ much from that if [^{3}H]-AZT was used. The distinction between the dynamics of AZT accumulation in dog and mouse blood after HpAZT administration could be explained by the differences in their metabolism. It is known that the blood turnover rate in mouse is only 7 s. Thus, one of the reasons of the reduced clinical toxicity of HpAZT could be the lower cellular concentration of AZT and AZTMP derived from HpAZT if compared with that derived from AZT.

Acknowledgements

We gratefully acknowledge Russian Foundation of Basic Research (Grant 02-04-49009), Russian Federation Ministry of Industry, Science, and Technology (AIDS, project N 31), and Presidium of Russian Academy of Sciences (Grant Physicochemical Biology) for financial support of this research. We are very thankful to Maxim Jasko for useful discussion.

References

Aggarwal, S.K., Gogu, S.R., Rangan, S.R.S., Agrawal, K.C., 1990. Synthesis and biological evaluation of progrugs of zidovudine. J. Med. Chem. 33, 1505–1510.

Balzarini, J., Hao, Z., Herdwijn, P., Johns, D.G., De Clercq, E., 1991. Intracellular metabolism and mechanism of anti-retrovirus action of 9-(2-phosphonylmethoxyethyl)adenine, a potent anti-human immunodeficiency virus compound. Proc. Natl. Acad. Sci. U.S.A. 88, 1499–1503.

Boal, J.H., Iyer, R.P., Egan, W., 1993. The 5′-hydrogenphosphonate analog as a potential prodrug of 3′-azido-2′, 3′-dideoxythymidine (AZT). Nucleosides & Nucleotides 12, 1075–1084.

Bonina, F., Puglia, C., Rimoli, M.G., Avallone, L., Abignente, E., Boatto, G., Nieddu, M., Meli, R., Amorena, M., De Caprariis, P., 2002. Synthesis and in vitro chemical and enzymatic stability of glycosyl 3′-azido-3′-deoxythymidine derivatives as potential anti-HIV agents. Eur. J. Pharm. Sci. 16, 167–174.

Chariot, P., Drogou, I., De Lacroix-Szmania, I., Eliezer-Vanerot, M.C., Chazaud, B., Lombes, A., Schaffer, A., Zafrani, E.S., 1999. Zidovudine-induced mitochondrial disorder with massive liver steatosis, myopathy, lactic acidosis, and mitochondrial DNA depletion. J. Hepatol. 30, 156–160.

Girard, P.M., Pegram, P.S., Diquet, B., Anderson, R., Raffi, F., Tubiana, R., Sereni, D., Boerner, D., 2000. Phase II placebo-controlled trial of fozivudine tidoxil for HIV infection: pharmacokinetics, tolerability, and efficacy. J. Acquir. Immune Defic. Syndr. 23, 227–235.

Gosselin, G., Perigaud, C., Lefebvre, I., Pompon, A., Aubertin, A.M., Kirn, A., Szabo, T., Stawinski, J., Imbach, J.L., 1993. 5′-hydrogenphosphonates of anti-HIV nucleoside analogues revisited: controversial mode of action. Antiviral Res. 22, 143–153.

Grootuis, D.R., Levy, R.M., 1997. The entry of antiviral and antiretroviral drugs into the central nervous system. J. Neurovirol. 3, 387–400.

Kellam, P., Boucher, C.A., Larder, B.A., 1992. Fifth mutations in HIV-1 resistance to zidovudine. Proc. Natl. Acad. Sci. U.S.A. 89, 1934–1938.

Khorlin, A.A., Tarusova, N.B., Dyatkina, N.B., Krayevsky, A.A., Biabialashvilli, R.Sh., Galegov, G.A., Zhdanov V.M., 1992. 5′-Phosphonates of 3′-azido-2′,3′-dideoxynucleosides are specific inhibitors of HIV reproduction in cell culture of H9/IIIB lymphocytes. Patent N 5043437, USA.

Klecker, R.W., Collins, J.M., Yarchoan, R., Thomas, R., Jenkins, J.R., Broder, S., Meyers, C.E., 1987. Plasma and cerebrospinal fluid pharmacokinetics of 3′-azido-3′-deoxythymidine: A novel pyrimidine analog with potential application for the treatment of patients with AIDS and related diseases. Clin. Pharmacol. Ther. 41, 407–412.

Kravchenko, A.V., Salamov, G.G., Bogoslovskaya, E.V., Serebrovskaya, L.V., Sergienko, O.G., Pokrovsky, V.V., 2001. Three-component combined antiretriviral therapy using HIV reverse transcriptase inhibitors. Epidemiol. Infect. Dis. (Russian) 4, 32–35.

Machado, J., Tsoukas, C., Salomon, H., Krayevsky, A., Wainberg M., 1999. Antiviral activity and resistance profile of phosphazid—a novel prodrug of AZT. In: Proceedings of the Sixth Conference on Retroviral and Opportunistic Infections. Chicago, USA, 31 January–4 February, 1999.

McGuigan, C., Devine, K.G., O'Conneor, T.J., Galpin, S.A., Jeffries, D.J., Kinchington, D., 1990. Synthesis and evaluation of some novel phosphoramidate derivatives of 3′-azido-3′-deoxythymidine (AZT) as anti-HIV compounds. Antiviral Chem. Chemother. 1, 107–113.

McGuigan, C., Cahard, D., Sheeka, H.M., De Clercq, E., Balzarini, J., 1996. Aryl phosphoramidate derivatives of d4T have improved anti-HIV efficacy in tissue culture and may act by the generation of a novel intracellular metabolite. J. Med. Chem. 39, 1748–1753.

Perigaud, C., Gosselin, G., Imbach, J.-L., 1997. Minireview: from the pronucleotide concept to the SATE phosphate protecting groups. Curr. Top. Med. Chem. 2, 15–29.

Piantadosi, C., Marasco, C.J., Morris-Natschke, S.L., Meyer, K.L., Gumus, F., Sures, J.R., Ishag, K.S., Kucera, S.L., Iyer, N., Wallen, C.A., Piantadosi, S., Modest, E.J., 1991. Synthesis and evaluation of novel lipid nucleoside conjugates for anti-HIV activity. J. Med. Chem. 34, 1408–1414.

Ren, J., Esnouf, R.M., Hopkins, A.L., Jones, E.Y., Kirby, L., Keeling, J., Ross, C.K., Larder, B.A., Stuart, D.I., Stammers, D.K., 1998. 3′-Azido-3′-deoxythymidine drug resistance mutations in HIV-1 reverse transcriptase can induce long-range conformational changes. Proc. Natl. Acad. Sci. U.S.A. 95, 9518–9523.

Richman, D.D., Fischl, M.A., Grieco, M.H., Gottlieb, M.S., Volberding, P.A., Laskin, O.L., Leedom, J.M., Groopman, J.E., Mildvan, D., Hirsch, M.S., Jackson, G.G., Duyack, D.T., Nusinoff-Lehrmann, S., 1987. The toxicity of azidothymidine in the treatment of patients with AIDS and AIDS-related complex. N. Engl. J. Med. 317, 192–197.

Sidorov, G.V., Zverkov, Yu.B., Myasoedov, N.F., Jasko, M.V., Skoblov, Yu.S., 2003. The synthesis of tritium-labelled 3′-azido-3′-deoxythymidine. J. Labelled Compd. Rad. 46, 1–8.

Tornevik, Y., Ullman, B., Balzarini, J., Wahren, B., Eriksson, S., 1995. Cytotoxicity of 3′-azido-3′-deoxythymidine correlates with 3′-azidothymidine-5′-monophosphate (AZTMP) levels, whereas anti-human immunodeficiency virus (HIV) activity correlates with 3′-azidothymidine-5′-triphosphate (AZTTP) levels in cultured CEM T-lymphoblastoid cells. Biochem. Pharmacol. 49, 829–837.

Vlieghe, P., Clerc, T., Pannecouque, C., Witvrouw, M., De Clercq, E., Salles, J.P., Kraus, J.L., 2001. New 3′-azido-3′-deoxythymidine-5′-yl O-4-hydroxyalkyl or alkenyl or alkylepoxide carbonate prodrugs: synthesis and anti-HIV evaluation. J. Med. Chem. 44, 3014–3021.

Wagner, C.R., Iyer, V.V., McIntee, E.J., 2000. Pronucleotides: toward the in vivo delivery of antiviral and anticancer nucleotides. Med. Res. Rev. 20, 417–451.

Wainberg, M., Krayevsky, A.A., Tarussova, N.B., Zhu, Q.Y., Vidal, P., Chou, T.C., Baron, P., Polsky, B., Jiang, X.J., Matulic-Adamic, J., Rosenberg, I., Watanabe, K.A., 1992. Hydrogenphosphonates and 5′-methylphosphonates of sugar modified pyrimidine nucleosides as potential anti-HIV agents. Nucleosides & Nucleotides 11, 177–196.

Wainberg, M.A., Gotte, M., Salomon, H., Quan, Y., 1998. Development of drug resistance following nucleoside treatment of HIV disease. Abstracts of the Thirteenth International Round Table on "Nucleosides, Nucleotides and their Biological Applications", Montpellier, France, 6–10 September, 1998.

Yurin, O.U., Krayevsky, A.A., Afonina, L.Yu., Balaganin, V.A., Burova, N.V., Voronin, E.E., Kolesnik, A.N., Molodov, I.B., Moshkovich, G.F., Pokrovsky, V.V., 2001. Phosphazid—new antiretroviral drug. Epidemiol. Infect. Dis. (Russian) 1, 43–45.

Yarchoan, R., Weinhold, K.J., Lyerly, H.K., Gelmann, E., Blum, R.M., Shearer, G.M., Mitsuya, H., Collins, J.M., Meyers, C.E., Klecker, R.W., Markhamn, P.D., Durack, D.T., Nusinoff-Lehrmann, S., Barry, D.W., Fischl, M.A., Gallo, R.C., Bolognesi, D.P., Broder, S., 1986. Administration of 3′-azido-3′-deoxythymidine, an inhibitor of HTLVIII/LAV replication, to patients with AIDS or AIDS related complex. Lancet I, 575–585.

Zemlicka, J., 2002. Lipophilic phosphoramidates as antiviral pronucleotides. Biochim. Biophys. Acta. 1587, 276–286.